

# Solitary Waves in a Five Component Dusty Plasma with Kappa described Electrons and Ions

Sijo Sebastian<sup>1</sup>, Sreekala G.<sup>2</sup>, Manesh Michael<sup>3</sup>, Noble P. Abraham<sup>4</sup>, S. Antony<sup>5</sup>, G. Renuka<sup>6</sup>, Chandu Venugopal<sup>7</sup>

<sup>1, 2, 3, 4, 5, 7</sup>School of Pure & Applied Physics, Mahatma Gandhi University,  
Priyadarshini Hills, Kottayam, 686 560, Kerala, India

<sup>6</sup>Kerala State Council for Science, Technology & Environment, Sasthra Bhavan, Pattom,  
Thiruvananthapuram, 695 004, Kerala, India

**Abstract:** *We investigate the existence of solitary waves in a five component dusty plasma. Positively and negatively charged dust, kappa function described photo-electrons, hot electrons and ions form the five components. The Kd-V equation is derived and the solutions plotted for different physical parameters. It is seen that different physical parameters affect the amplitude of the solitary structures differently. As the temperature of negative dust increases, the amplitude of the solitary structure increases. With the increase of positive dust number densities, the amplitude of the solitary structure decreases whereas its amplitude increases with an increase of hydrogen ion densities.*

**Keywords:** Solitary waves, Five component Dusty Plasma, Kappa distributed ions and electrons, Kd-V equation, Soliton

## 1. Introduction

Dusty plasmas, which play a significant role in space, astrophysical and laboratory environments, is an interesting current field of research because dust significantly alters the charged particles' equilibrium density leading to different phenomena. Dust is widespread in the plasmas of cometary tails, asteroid zones, rings of Saturn, interstellar clouds and the Earth's magnetosphere [1-4].

This omnipresent dust makes nonlinear studies in plasmas very complex and extremely important, and phenomena like solitons, shocks and vortices have been investigated in great detail [5]. Also the discovery of the existence of new eigen modes like Dust-Acoustic Waves (DAWs) [6], Dust Ion-Acoustic Waves (DIAWs) [7] and Dust Lattice Waves (DLWs) [8] have given a new dimension to the study of dusty plasmas. Most of the dusty plasma studies, until recently, considered only negatively charged dust as a constituent [9-12].

However, many authors have found different environments where both positively and negatively charged dust could exist. In particular, it was shown by Ellis and Neff [10] that the sign of the charge on the dust grains in the tail of comet Halley is a function of distance. Similarly, it was shown that the grain potential could be either positive or negative in the region between the outer shock and the cometary ionopause [1]. Also, as shown by Chow et. al. [11], typical cosmic plasmas have grains of different sizes of opposite charge: the smaller ones were positively charged while larger sized grains were negatively charged. Nearer Earth, Havnes et. al. [13], analyzing data from two rockets launched from the Audoya Rocket Range, found that the negative charge density locked in the dust grains was so large that an electron bite out was the result. And the increase in the local electron density by photoionization resulted in positively charged dust grains.

Thus there are a number of space, astrophysical and cosmic plasmas that carry both positively and negatively charged dust grains.

Recently, Voelzke and Izaguirre analysed 886 images of the comet Halley and found 41 solitary waves (solitons) in addition to other wavy structures [14].

Dust – acoustic solitary waves in unmagnetized three component dusty plasmas consisting of ions, electrons and negatively charged dust have been studied by many authors [9, 15, 16]. However, with the realization of the importance of the presence of positively charged dust, researchers turned their attention to four-component plasmas consisting of ions, electrons and positively and negatively charged dust. Thus Sayed and Mamun [17] investigated solitary waves in a four component dusty plasma using the reductive perturbation technique [RPT]; a complementary study using the Sagdeev potential technique was carried by Chatterjee and Roy [18]. This wave has also been studied in a four component adiabatic, magnetized plasma [19].

Plasmas observed in different space environments deviate significantly from the well known Maxwellian distribution due to the presence of the high energy particles in the tail of the distribution. Using solar wind data Vasyliunas first predicted a non-Maxwellian distribution [20]; this distribution, which subsequently came to be known as the “kappa distribution”, has been found in many magnetospheric and astrophysical environments. Acoustic-like solitary waves, with the electrons described by kappa distributions, have been studied by many authors recently [21-26]. Linear and nonlinear waves in dusty plasmas, where both ions and electrons are described by kappa distributions, have also been studied [27-28].

A realistic model of a cometary plasma requires at least five components: in addition to solar wind protons and electrons, the dissociation of water group molecules would give rise to

positively charged oxygen ions and the associated photo-electrons ( the second colder, electron component) [29]. And the unexpected discovery of negatively charged oxygen ions in a cometary plasma is now well known [30].

We thus investigate the existence of solitary waves in a five component plasma: positively charged oxygen ions (dust), negatively charged oxygen ions (dust), hydrogen ions, hotter solar wind electrons and colder photo-electrons. And for reasons we model the hydrogen ions and electrons by kappa distributions

## 2. Basic equations

We are interested in solitary waves in a five constituent plasma, for reasons given above. The dust components are treated as cold, while the other three constituents are described by a Boltzmann-like distribution given by

$$n_s = n_{s0} \left[ 1 + \frac{e_s \psi}{k_B T_s (\kappa_s - 1/2)} \right]^{-\kappa_s + 1/2}; s = H, se, ce \quad (1)$$

In (1)  $s$  indicates the species ( $s = H$  for hydrogen,  $s = se$  for solar electrons and  $s = ce$  for cometary photo-electrons).  $n$  denotes the density (with the subscript '0' denoting the equilibrium value),  $e_s$  the charge,  $T_s$  the temperature and  $\kappa_s$  the spectral index for the species ' $s$ '.  $k_B$  is the Boltzmann's constant and  $\psi$ , is the potential.

The normalized form of the two continuity equations and the equations of motion for the dust particles and the Poisson's equation are thus given by

$$\frac{\partial n_1}{\partial t} + \frac{\partial(n_1 u_1)}{\partial x} = 0 \quad (2)$$

$$\frac{\partial u_1}{\partial t} + u_1 \frac{\partial u_1}{\partial x} = \frac{\partial \psi}{\partial x} \quad (3)$$

$$\frac{\partial n_2}{\partial t} + \frac{\partial(n_2 u_2)}{\partial x} = 0 \quad (4)$$

$$\frac{\partial u_2}{\partial t} + u_2 \frac{\partial u_2}{\partial x} = -\alpha \beta \frac{\partial \psi}{\partial x} \quad (5)$$

$$\begin{aligned} \frac{\partial^2 \psi}{\partial x^2} = & n_1 - (1 - \mu_i + \mu_{se} + \mu_{ce}) n_2 \\ & + \mu_{se} \left( 1 - \frac{\psi}{\sigma_{se} (\kappa_{se} - 1/2)} \right)^{(-\kappa_{se} + 1/2)} \\ & + \mu_{ce} \left( 1 - \frac{\psi}{\sigma_{ce} (\kappa_{ce} - 1/2)} \right)^{(-\kappa_{ce} + 1/2)} \\ & - \mu_i \left( 1 + \frac{\psi}{\sigma_i (\kappa_i - 1/2)} \right)^{(-\kappa_i + 1/2)} \end{aligned} \quad (6)$$

In (2) to (6)  $n_1$  and  $n_2$  are the negative and positive dust number densities, normalized by their equilibrium values

$n_{10}$  and  $n_{20}$  respectively.  $u_1$  and  $u_2$  are, respectively, the negatively and positively charged dust fluid speeds normalized by  $\frac{z_1 k_B T_1}{m_1}$ .  $\psi$ , which is now the normalized

electric potential, is normalized by  $\frac{k_B T_1}{e}$ .  $x$  and  $t$  are

normalized by the Debye length  $\lambda_D = \left( \frac{z_1 k_B T_1}{4\pi z_1 e^2 n_{10}} \right)^{1/2}$  and

the inverse of the plasma frequency  $\omega_{p1}^{-1} = \left( \frac{m_1}{4\pi z_1 e^2 n_{10}} \right)^{1/2}$

respectively. Also  $\alpha = \frac{z_2}{z_1}$ ,  $\beta = \frac{m_1}{m_2}$ ,  $\mu_s = \frac{n_{s0}}{z_1 n_{10}}$ ,  $\sigma_s = \frac{T_s}{T_1}$

where  $n_{s0}$  is the equilibrium density for species  $s$ .  $T_s$  and  $T_1$  are the temperatures of species  $s$  and negative dust respectively.  $m_1$  and  $m_2$  are, respectively, the masses of negatively and positively charged dust particles while  $z_1$  and  $z_2$  are the corresponding charge numbers.

To derive Kd-V equations of small amplitude waves, we introduce a new variables  $\xi$  and  $\tau$  as:

$$\xi = \varepsilon^{1/2} (X - Mt)$$

$$\tau = \varepsilon^{3/2} t.$$

By the substitution  $\frac{\partial}{\partial x} = \varepsilon^{1/2} \frac{\partial}{\partial \xi}$  and

$$\frac{\partial}{\partial t} = \varepsilon^{3/2} \frac{\partial}{\partial \tau} - \varepsilon^{1/2} M \frac{\partial}{\partial \xi}, \quad (2) - (5) \text{ become}$$

$$\varepsilon^{3/2} \frac{\partial n_1}{\partial \tau} - \varepsilon^{1/2} M \frac{\partial n_1}{\partial \xi} + \varepsilon^{1/2} \frac{\partial(n_1 u_1)}{\partial \xi} = 0 \quad (7)$$

$$\varepsilon^{3/2} \frac{\partial u_1}{\partial \tau} - \varepsilon^{1/2} M \frac{\partial u_1}{\partial \xi} + \varepsilon^{1/2} u_1 \frac{\partial u_1}{\partial \xi} = \varepsilon^{1/2} \frac{\partial \psi}{\partial \xi} \quad (8)$$

$$\varepsilon^{3/2} \frac{\partial n_2}{\partial \tau} - \varepsilon^{1/2} M \frac{\partial n_2}{\partial \xi} + \varepsilon^{1/2} \frac{\partial(n_2 u_2)}{\partial \xi} = 0 \quad (9)$$

$$\varepsilon^{3/2} \frac{\partial u_2}{\partial \tau} - \varepsilon^{1/2} M \frac{\partial u_2}{\partial \xi} + \varepsilon^{1/2} u_2 \frac{\partial u_2}{\partial \xi} = -\varepsilon^{1/2} \alpha \beta \frac{\partial \psi}{\partial \xi} \quad (10)$$

The physical quantities in the above equations can be expressed asymptotically as a power in  $\varepsilon$  about equilibrium state as:

$$n_1 = 1 + \varepsilon n_1^{(1)} + \varepsilon^2 n_1^{(2)} + \dots \quad (11)$$

$$n_2 = 1 + \varepsilon n_2^{(1)} + \varepsilon^2 n_2^{(2)} + \dots \quad (12)$$

$$u_1 = 0 + \varepsilon u_1^{(1)} + \varepsilon^2 u_1^{(2)} + \dots \quad (13)$$

$$u_2 = 0 + \varepsilon u_2^{(1)} + \varepsilon^2 u_2^{(2)} + \dots \quad (14)$$

$$\psi = \varepsilon \psi^{(1)} + \varepsilon^2 \psi^{(2)} + \dots \quad (15)$$

Substituting above equations in (7)-(10) and equating powers of  $\varepsilon^{3/2}$ , we get

$$n_1^{(1)} = \frac{u_1^{(1)}}{M}, \quad n_2^{(1)} = \frac{u_2^{(1)}}{M} \quad (16)$$

$$u_1^{(1)} = \frac{-\psi^{(1)}}{M} \quad \text{and} \quad u_2^{(1)} = \frac{\alpha\beta}{M} \psi^{(1)} \quad (17)$$

Similarly equating power of  $\varepsilon$  from equation (6), we get as

$$0 = n_1^{(1)} - n_2^{(1)} (1 - \mu_i + \mu_{se} + \mu_{ce}) + \frac{\mu_{se}}{\sigma_{se}} \left\{ \frac{(\kappa_{se} - 1/2)}{(\kappa_{se} - 3/2)} \right\} \psi^{(1)} + \frac{\mu_{ce}}{\sigma_{ce}} \left\{ \frac{(\kappa_{ce} - 1/2)}{(\kappa_{ce} - 3/2)} \right\} \psi^{(1)} + \frac{\mu_i}{\sigma_i} \left\{ \frac{(\kappa_i - 1/2)}{(\kappa_i - 3/2)} \right\} \psi^{(1)} \quad (18)$$

Using equation (17), we can write equation (16) as

$$n_1^{(1)} = \frac{-\psi^{(1)}}{M^2} \quad \text{and} \quad n_2^{(1)} = \frac{\alpha\beta\psi^{(1)}}{M^2} \quad (19)$$

With the use of above equation, (19) can be written as

$$M^2 = \frac{1 + \alpha\beta(1 - \mu_i + \mu_{se} + \mu_{ce})}{\frac{\mu_{se}}{\sigma_{se}} \left\{ \frac{(\kappa_{se} - 1/2)}{(\kappa_{se} - 3/2)} \right\} + \frac{\mu_{ce}}{\sigma_{ce}} \left\{ \frac{(\kappa_{ce} - 1/2)}{(\kappa_{ce} - 3/2)} \right\} + \frac{\mu_i}{\sigma_i} \left\{ \frac{(\kappa_i - 1/2)}{(\kappa_i - 3/2)} \right\}} \quad (20)$$

Similarly equating powers of  $\varepsilon^{3/2}$  from equations (7)-(10) and  $\varepsilon^2$  from equation (6), we get

$$\frac{\partial n_1^{(1)}}{\partial \tau} - M \frac{\partial n_1^{(2)}}{\partial \xi} + \frac{\partial u_1^{(2)}}{\partial \xi} + \frac{\partial(n_1^{(1)} u_1^{(1)})}{\partial \xi} = 0 \quad (21)$$

$$\frac{\partial n_2^{(1)}}{\partial \tau} - M \frac{\partial n_2^{(2)}}{\partial \xi} + \frac{\partial u_2^{(2)}}{\partial \xi} + \frac{\partial(n_2^{(1)} u_2^{(1)})}{\partial \xi} = 0 \quad (22)$$

$$\frac{\partial u_1^{(1)}}{\partial \tau} - M \frac{\partial u_1^{(2)}}{\partial \xi} + u_1^{(1)} \frac{\partial u_1^{(1)}}{\partial \xi} = \frac{\partial \psi^{(2)}}{\partial \xi} \quad (23)$$

$$\frac{\partial u_2^{(1)}}{\partial \tau} - M \frac{\partial u_2^{(2)}}{\partial \xi} + u_2^{(1)} \frac{\partial u_2^{(1)}}{\partial \xi} = -\alpha\beta \frac{\partial \psi^{(2)}}{\partial \xi} \quad (24)$$

$$\begin{aligned} \frac{\partial^2 \psi^{(1)}}{\partial \xi^2} = & n_1^{(2)} - n_2^{(2)} (1 - \mu_i + \mu_{se} + \mu_{ce}) \\ & + \frac{\mu_{se}}{\sigma_{se}} \left\{ \frac{(\kappa_{se} - 1/2)}{(\kappa_{se} - 3/2)} \right\} \psi^{(2)} + \frac{\mu_{ce}}{\sigma_{ce}} \left\{ \frac{(\kappa_{ce} - 1/2)}{(\kappa_{ce} - 3/2)} \right\} \psi^{(2)} \\ & + \frac{\mu_i}{\sigma_i} \left\{ \frac{(\kappa_i - 1/2)}{(\kappa_i - 3/2)} \right\} \psi^{(2)} + \frac{\mu_{se}}{2\sigma_{se}^2} \left\{ \frac{(\kappa_{se} - 1/2)(\kappa_{se} + 1/2)}{(\kappa_{se} - 3/2)^2} \right\} \psi^{(1)2} \\ & + \frac{\mu_{ce}}{2\sigma_{ce}^2} \left\{ \frac{(\kappa_{ce} - 1/2)(\kappa_{ce} + 1/2)}{(\kappa_{ce} - 3/2)^2} \right\} \psi^{(1)2} - \frac{\mu_i}{2\sigma_i^2} \left\{ \frac{(\kappa_i - 1/2)(\kappa_i + 1/2)}{(\kappa_i - 3/2)^2} \right\} \psi^{(1)2} \end{aligned} \quad (25)$$

Using equations (17), (18), (19), (21), (22), (23) and (24), we can write above equation as

$$\frac{\partial \psi^{(1)}}{\partial \tau} + A \psi^{(1)} \frac{\partial \psi^{(1)}}{\partial \xi} + B \frac{\partial^3 \psi^{(1)}}{\partial \xi^3} = 0$$

Where

$$A = \frac{1}{2M(1 + \alpha\beta(1 - \mu_i + \mu_{se} + \mu_{ce}))} \{ [3\alpha^2\beta^2(1 - \mu_i + \mu_{se} + \mu_{ce}) - 3] - M^4 \left[ \frac{\mu_{se}}{\sigma_{se}^2} \left\{ \frac{(\kappa_{se} - 1/2)(\kappa_{se} + 1/2)}{(\kappa_{se} - 3/2)^2} \right\} + \frac{\mu_{ce}}{\sigma_{ce}^2} \left\{ \frac{(\kappa_{ce} - 1/2)(\kappa_{ce} + 1/2)}{(\kappa_{ce} - 3/2)^2} \right\} - \frac{\mu_i}{\sigma_i^2} \left\{ \frac{(\kappa_i - 1/2)(\kappa_i + 1/2)}{(\kappa_i - 3/2)^2} \right\} \right] \} \}$$

$$B = \frac{M^3}{2(1 + \alpha\beta(1 - \mu_i + \mu_{se} + \mu_{ce}))}$$

### 3. Solution of Kd-V Equation

For the solution of the Kd-V equation, we follow the method of Kolebaga and Oyewande [31]. For this we use the transformation  $\psi^{(1)} = f(\xi - U\tau) = f(\chi)$ .

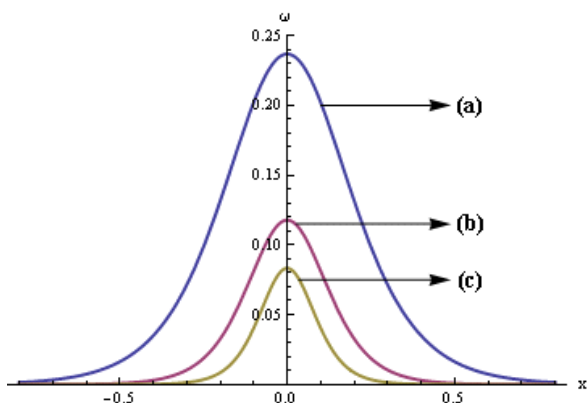
Finally we can arrive at the solution of Kd-V equation as

$$\psi = \psi_m \text{sech}^2 \left( \frac{\chi_0 - \chi}{\omega} \right)$$

where  $\psi_m = \frac{3U}{A}$  is the amplitude and  $\omega = 2\sqrt{\frac{B}{U}}$  is the width of the solitons.

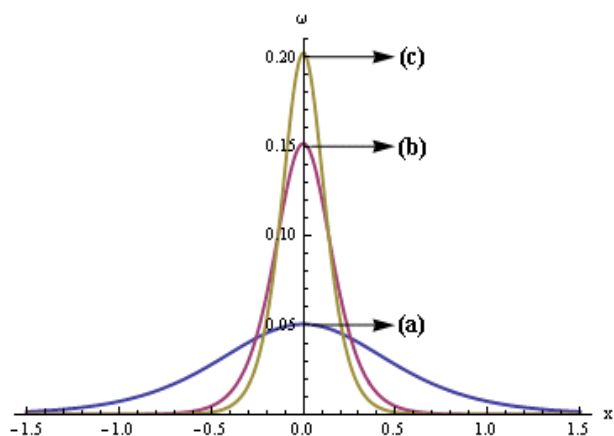
### 3. Discussions

Though our equations are valid for arbitrary values of charge numbers  $z_1$  and  $z_2$  on the dust particles we are interested, in this paper, on parameters relevant to comet Halley. The density of hydrogen ions observed at comet Halley was  $4.95 \text{ cm}^{-3}$  at a temperature of  $8 \times 10^4 \text{ K}$ . The solar electron temperature was  $2 \times 10^5 \text{ K}$  [29]. The negatively charged ions were detected at an energy of 1 eV, with densities  $\leq 1 \text{ cm}^{-3}$  in the 7-19 amu peak [30]. Therefore we choose a majority ion density  $n_{i0} = 4.95 \text{ cm}^{-3}$  and temperature  $T_i = 8 \times 10^4 \text{ K}$ , hot electron temperature  $T_{se} = 2 \times 10^5 \text{ K}$  and photo-electron temperature  $T_{ce} = 2 \times 10^4 \text{ K}$ . Negatively and positively charged oxygen ions are considered in lieu of negatively and positively charged dust with densities of  $n_{10} = 0.05 \text{ cm}^{-3}$  and  $n_{20} = 0.5 \text{ cm}^{-3}$  respectively. The temperature of negatively and positively charged oxygen is taken as  $T_1 = 1.16 \times 10^4 \text{ K}$  [30].



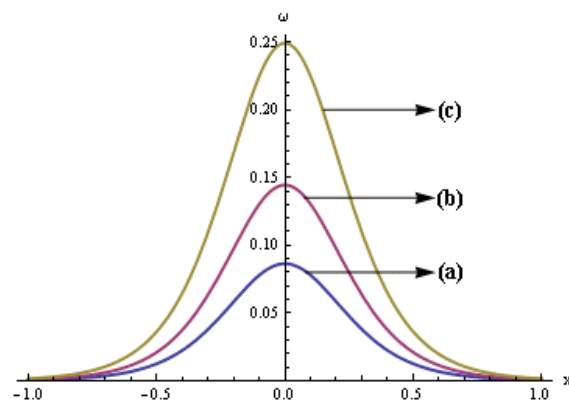
**Figure 1:** Plots of  $\psi$  vs.  $x$  for different  $z_2$  values. Curve (a) is for  $z_2 = 4$ , (b) for  $z_2 = 5$  and (c) for  $z_2 = 6$ .

Figure 1 shows the plot of  $\psi$  vs.  $x$  for different  $z_2$  values. Curve (a) is for  $z_2 = 4$ , (b) for  $z_2 = 5$  and (c) for  $z_2 = 6$ . The other parameters are  $M = 2$ ,  $U = 0.1$ ,  $n_{10} = 0.05 \text{ cm}^{-3}$ ,  $n_{20} = 0.5 \text{ cm}^{-3}$ ,  $n_{i0} = 4.95 \text{ cm}^{-3}$ ,  $T_{ce} = 2 \times 10^4 \text{ K}$ ,  $T_{se} = 2 \times 10^5 \text{ K}$ ,  $T_i = 8 \times 10^4 \text{ K}$ ,  $T_1 = 1.16 \times 10^4 \text{ K}$ ,  $z_1 = 1$ ,  $\kappa_{ce} = \kappa_i = 4$  and  $\kappa_{se} = 12$ . It is seen that as the  $z_2$  increases, amplitude of the solitary wave decreases.



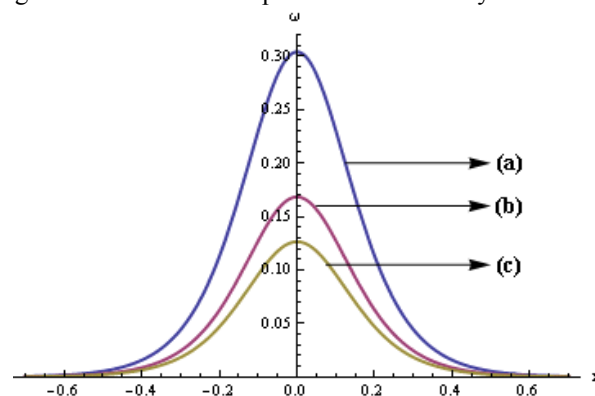
**Figure 2:** Plots of  $\psi$  vs.  $x$  for different  $U$  values. Curve (a) is for  $U = 0.03$ , (b) for  $U = 0.09$  and (c) for  $U = 0.12$ .

Figure 2 shows the plot of  $\psi$  vs.  $x$  for different  $U$  values. Curve (a) is for  $U = 0.03$ , (b) for  $U = 0.09$  and (c) for  $U = 0.12$ . The other parameters are  $M = 1.5$ ,  $n_{10} = 0.05 \text{ cm}^{-3}$ ,  $n_{20} = 0.5 \text{ cm}^{-3}$ ,  $n_{i0} = 4.95 \text{ cm}^{-3}$ ,  $T_{ce} = 2 \times 10^4 \text{ K}$ ,  $T_{se} = 2 \times 10^5 \text{ K}$ ,  $T_i = 8 \times 10^4 \text{ K}$ ,  $T_1 = 1.16 \times 10^4 \text{ K}$ ,  $z_1 = 1$ ,  $z_2 = 3$ ,  $\kappa_{ce} = \kappa_i = 4$  and  $\kappa_{se} = 12$ . It is seen that as the  $U$  increases, amplitude of the solitary wave increases significantly.



**Figure 3:** Plots of  $\psi$  vs.  $x$  for different  $T_1$  values. Curve (a) is for  $T_1 = 1 \times 10^4 \text{ K}$ , (b) for  $T_1 = 1.4 \times 10^4 \text{ K}$  and (c) for  $T_1 = 1.6 \times 10^4 \text{ K}$ .

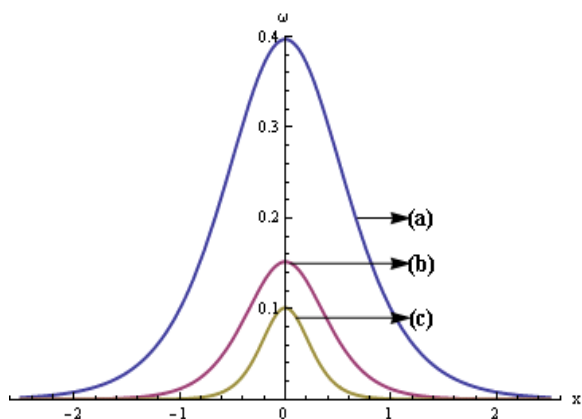
Figure 3 shows the plot of  $\psi$  vs.  $x$  for different  $T_1$  values. Curve (a) is for  $T_1 = 1 \times 10^4 \text{ K}$ , (b) for  $T_1 = 1.4 \times 10^4 \text{ K}$  and (c) for  $T_1 = 1.6 \times 10^4 \text{ K}$ . The other parameters are  $M = 1.5$ ,  $U = 0.06$ ,  $n_{10} = 0.05 \text{ cm}^{-3}$ ,  $n_{20} = 0.5 \text{ cm}^{-3}$ ,  $n_{i0} = 4.95 \text{ cm}^{-3}$ ,  $T_{ce} = 2 \times 10^4 \text{ K}$ ,  $T_{se} = 2 \times 10^5 \text{ K}$ ,  $T_i = 8 \times 10^4 \text{ K}$ ,  $z_1 = 1$ ,  $z_2 = 3$ ,  $\kappa_{ce} = \kappa_i = 4$  and  $\kappa_{se} = 12$ . From the graph, it is clear that as the negative dust temperature increases, the amplitude of the solitary structure increases; i.e. negative dust temperature has a significant role in the amplitude of the solitary structures.



**Figure 4:** Plots of  $\psi$  vs.  $x$  for different  $\kappa_{ce} = \kappa_i$  values.

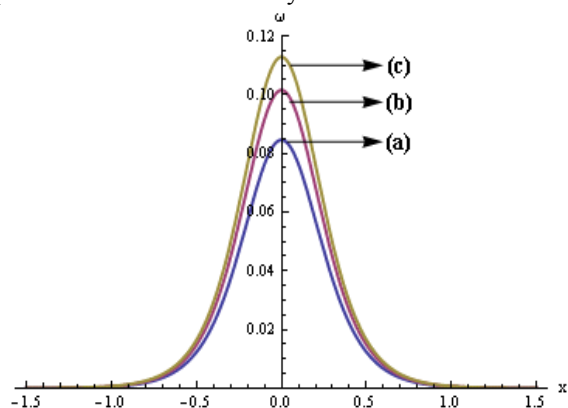
Curve (a) is for  $\kappa_{ce} = \kappa_i = 3$ , (b) for  $\kappa_{ce} = \kappa_i = 4$  and (c) for  $\kappa_{ce} = \kappa_i = 9$ .

Figure 4 shows the plot of  $\psi$  vs.  $x$  for different  $\kappa_{ce} = \kappa_i$  values. Curve (a) is for  $\kappa_{ce} = \kappa_i = 3$ , (b) for  $\kappa_{ce} = \kappa_i = 4$  and (c) for  $\kappa_{ce} = \kappa_i = 9$ . The other parameters are  $M = 1.5$ ,  $U = 0.1$ ,  $n_{10} = 0.05 \text{ cm}^{-3}$ ,  $n_{20} = 0.5 \text{ cm}^{-3}$ ,  $n_{i0} = 4.95 \text{ cm}^{-3}$ ,  $T_{ce} = 2 \times 10^4 \text{ K}$ ,  $T_{se} = 2 \times 10^5 \text{ K}$ ,  $T_i = 8 \times 10^4 \text{ K}$ ,  $z_1 = 1$ ,  $z_2 = 3$  and  $\kappa_{se} = 12$ . As kappa value increases, amplitude of the solitary structures decreases. There is only a slight change in the amplitude for higher values of kappa.



**Figure 5:** Plots of  $\psi$  vs.  $x$  for different  $n_{20}$  values. Curve (a) is for  $n_{20} = 0.2$ , (b) for  $n_{20} = 0.3$  and (c) for  $n_{20} = 0.5$ .

Figure 5 shows the plot of  $\psi$  vs.  $x$  for different  $n_{20}$  values. Curve (a) is for  $n_{20} = 0.2$ , (b) for  $n_{20} = 0.3$  and (c) for  $n_{20} = 0.5$ .  $T_1$  is taken as  $1.16 \times 10^4 K$ . Other relevant parameters are same as figure 3. From the graph, we can see that amplitude of the solitary waves decreases with increase of positive dust number density.



**Figure 6:** Plots of  $\psi$  vs.  $x$  for different  $n_{i0}$  values. Curve (a) is for  $n_{i0} = 3$ , (b) for  $n_{i0} = 5$  and (c) for  $n_{i0} = 6$ .

Figure 6 shows the plot of  $\psi$  vs.  $x$  for different  $n_{i0}$  values. Curve (a) is for  $n_{i0} = 0.2$ , (b) for  $n_{i0} = 0.3$  and (c) for  $n_{i0} = 0.5$ .  $n_{20}$  is taken as  $0.5$ . Other values remain the same as in the previous case. From the graph, it is seen that amplitude of the solitary structures increases with increase of hydrogen ion densities.

#### 4. Conclusions

We have studied solitary wave propagation in a five component dusty plasma consisting of kappa described electrons, hot electrons and ions and also negatively and positively charged oxygen ions. Solitary structures are obtained from Kd-V equations. Different physical parameter affect differently in the amplitude of the solitary structures obtained from the Kd-V equation. As the negative charge number increases amplitude of the solitary wave increases, but the opposite happens in the case of addition of positive

charge numbers. Positive dust number density has adverse effect in the solitary structures i.e. amplitude of the solitary structure decreases with the increase of density whereas amplitude increases with an increase of hydrogen ion density.

#### 5. Acknowledgment

Financial assistance from DST (FIST and PURSE), KSCSTE, Thiruvananthapuram and UGC (EF and SAP) is gratefully acknowledged.

#### References

- [1] M. Horányi and D.A. Mendis, "Trajectories Of Charged Dust Grains In The Cometary Environment," *Astrophys. J.* 294, 357 (1985)
- [2] P. K. Shukla, "A Survey Of Dusty Plasma Physics," *Phys. Plasmas* 8, 1791 (2001)
- [3] P. K. Shukla and A. A. Mamun, "Introduction To Dusty Plasma Physics," Institute of Physics, Bristol (2002)
- [4] A. A. Mamun and P. K. Shukla, "Solitary Potentials In Cometary Dusty Plasmas," *Geophys. Res. Lett.* 29, 1870 (2002)
- [5] P. K. Shukla and A. A. Mamun, "Solitons, Shocks And Vortices In Dusty Plasmas," *New J. Phys.* 5, 17 (2003)
- [6] N. N. Rao, P. K. Shukla and M.Y. Yu, "Dust-acoustic waves in dusty plasmas," *Planet. Space Sci.* 38 543 (1990)
- [7] P. K. Shukla and V. P. Silin, "Dust Ion-Acoustic Wave," *Phys. Scr.* 45 508 (1992)
- [8] F. Melandso, "Lattice Waves In Dust Plasma Crystals," *Phys. Plasmas* 3 3890 (1996)
- [9] P. Chatterjee and R. K. Jana, "Speed And Shape Of Dust Acoustic Solitary Waves In The Presence Of Dust Streaming," *Z. Naturforsch* 60 a 275 (2005)
- [10] T. A. Ellis and J. S. Neff, "Numerical Simulation Of The Emission And Motion Of Neutral And Charged Dust From P/Halley," *Icarus* 91 280 (1991)
- [11] V. W. Chow, D. A. Mendis and M. Rosenberg, "Role Of Grain Size And Particle Velocity Distribution In Secondary Electron Emission In Space Plasmas," *J. Geophys. Res.* 98 19065 (1993)
- [12] M. Horányi, G. E. Morfill and E. Grün, "Mechanism For The Acceleration And Ejection Of Dust Grains From Jupiter's Magnetosphere," *Nature* 363 144 (1993)
- [13] O. Havnes et. al., "First Detection Of Charged Dust Particles In The Earth's Mesosphere," *J. Geophys. Res.* 101 10839 (1996)
- [14] M. R. Voelzke And L. S. Izaguirre, "Morphological Analysis Of The Tail Structures Of Comet P/Halley 1910 II," *Planet. Space Sci.* 65 104 (2012)
- [15] S. Maitra and R. Roychoudhary, "Speed And Shape Of Dust Acoustic Solitary Waves," *Phys. Plasmas* 10 2230 (2003)
- [16] S. Mahmood and H. Saleem, "Dust Acoustic Solitary Wave In The Presence Of Dust Streaming," *Phys. Plasmas* 10 47 (2003)
- [17] F. Sayed and A. A. Mamun, "Solitary Potential In A Four-Component Dusty Plasma," *Phys. Plasmas* 14 014501 (2007)



- [17] P. Chatterjee and K. Roy, "Large Amplitude Solitary Waves In A Four-Component Dusty Plasma With Nonthermal Ions," *Z. Naturforsch* 63a 393 (2008)
- [18] T. Akhter, A. Mannan and A. A. Mamun, "Dust Acoustic Solitary Waves In A Four Component Adiabatic Magnetized Dusty Plasma," *Plasma Phys. Rep.* 13 548 (2013)
- [19] V. M. Vasyliunas, "A Survey Of Low-Energy Electrons In The Evening Sector Of The Magnetosphere With OGO 1 And OGO 3," *J. Geophys. Res.* 73 2839 (1968)
- [20] B. Basu, "Low Frequency Electrostatic Waves In Weakly Inhomogeneous Magnetoplasma Modeled By Lorentzian (Kappa) Distributions," *Phys. Plasmas* 15 042108 (2008)
- [21] T. K. Baluku and M. A. Hellberg, "Dust Acoustic Solitons In Plasmas With Kappa-Distributed Electrons And/Or Ions," *Phys. Plasmas* 15 123705 (2008)
- [22] N. S. Saini, I. Kourakis and M. A. Hellberg, "Arbitrary Amplitude Ion-Acoustic Solitary Excitations In The Presence Of Excess Superthermal Electrons," *Phys. Plasmas* 16 062903 (2009)
- [23] B. Sahu, "Electron Acoustic Solitary Waves And Double Layers With Superthermal Hot Electrons," *Phys. Plasmas* 17 122305 (2010)
- [24] A. Shah, S. Mahmood and Q. Haque, "Propagation Of Solitary Waves In Relativistic Electron-Positron-Ion Plasmas With Kappa Distributed Electrons And Positrons," *Phys. Plasmas* 18 114501 (2011)
- [25] C. R. Choi, K. W. Min and T. N. Rhee, "Electrostatic Korteweg-Devries Solitary Waves In A Plasma With Kappa-Distributed Electrons," *Phys. Plasmas* 18 092901(2011)
- [26] W. Masood and A. Ahmad, "Coupled Dispersive Drift Acoustic Modes In Inhomogeneous Dusty Plasmas With Different Nonthermal Distributions For Electrons And Ions," *Astrophys. Space Sci.* 340 367 (2012)
- [27] H. Haque, "Dust Drift Solitary Waves With Superthermal Electrons And Ions," *Astrophys. Space Sci.* 343 605 (2013)
- [28] A. L. Brinca and B. T. Tsurutani, "Unusual Characteristics Of The Electromagnetic Waves Excited By Cometary Newborn Ions With Large Perpendicular Energies," *Astron. Astrophys.* 187 311 (1987)
- [29] P. Chaizy et. al., "Negative Ions In The Coma Of Comet Halley," *Nature* 349 393 (1991)
- [30] O. Kolebaje and O. Oyewande, "Numerical Solution of the Korteweg De Vries Equation by Finite Difference and Adomian Decomposition Method," *International Journal of Basic and Applied Science* 1,321-335 (2012)